



Research articles

Temperature-dependent magnetization reversal in exchange bias NiFe/IrMn/NiFe structures



Ch. Gritsenko^{a,*}, I. Dzhun^b, M. Volochaev^c, M. Gorshenkov^d, G. Babaytsev^b, N. Chechenin^{b,e}, A. Sokolov^c, Oleg A. Tretiakov^{f,g,d}, V. Rodionova^{a,d}

^a Immanuel Kant Baltic Federal University, A. Nevskogo 14, 236041 Kaliningrad, Russia

^b Skobeltsyn Institute of Nuclear Physics, Lomonosov Moscow State University, Leninskie Gory 1/2, 119991 Moscow, Russia

^c Kirensky Institute of Physics, Federal Research Center KSC SB RAS, Akademgorodok 50/38, Krasnoyarsk 660036, Russia

^d National University of Science and Technology MISIS, Leninsky Prospekt 4, Moscow 119049, Russia

^e Faculty of Physics, Lomonosov Moscow State University, Leninskie Gory 1/2, 119991 Moscow, Russia

^f School of Physics, The University of New South Wales, Sydney 2052, Australia

^g Institute for Materials Research and Center for Science and Innovation in Spintronics, Tohoku University, Sendai 980-8577, Japan

ARTICLE INFO

Keywords:

Magnetization reversal
Exchange bias
Permalloy

ABSTRACT

We demonstrate magnetization reversal features in NiFe/IrMn/NiFe thin-film structures with 40% and 75% relative content of Ni in Permalloy in the temperature range from 80 K to 300 K. The magnetization reversal sequence of the two ferromagnetic layers is found to depend on the type of NiFe alloy. In the samples with 75% relative content of Ni, the bottom ferromagnetic layer reverses prior to the top one. On the contrary, in the samples with 40% of Ni, the top ferromagnetic layer reverses prior to the bottom one. These tendencies of magnetization reversal are preserved in the entire range of temperatures. These distinctions can be explained by the morphological and structural differences of interfaces in the samples based on two types of Permalloy.

1. Introduction

The exchange bias phenomenon can be observed in a system of adjacent antiferromagnetic (AFM) and ferromagnetic (FM) layers under the condition of an induced uniaxial magnetic anisotropy [1]. It leads to a shift of the hysteresis loop along the field axis. Along a fixed direction, the ferromagnetic layer becomes harder for magnetization reversal due to the exchange coupling interaction with the antiferromagnetic layer. As a result, the FM-layer is considered as a pinned layer, which is widely used in spin valves [2–5], magnetic sensors [6], and MRAM [7]. Depending on an application, the most important features of magnetization reversal process can be either the magnitude of the exchange bias [8,9] or sequence of ferromagnetic layers magnetization switching [10,11], reflected in peculiarities of hysteresis loops shape. The material parameters and characteristic

properties of the exchange-coupled systems influence the aforementioned features.

The exchange bias phenomenon has been confirmed to have a strong dependence on the types of FM and AFM materials. Commonly used in exchange bias systems ferromagnetic materials are Ni [12–14], Co [15,16], Fe [17,18], their alloys [19–21], and the alloys doped with impurities of elements, such as Pt [22,23]. Depending on magnetization and magnetic anisotropy of these FM materials [18,24–26], one can find different exchange bias and coercivity values for a required application [27–29]. In comparison with other ferromagnetic materials, NiFe alloys have small coercivity, high initial and maximum magnetic permeabilities, as well as corrosion resistance that can be useful for digital memory devices [30,31]. On the phase diagram of NiFe alloys one can distinguish two types of Permalloy depending on the Ni content, ‘low-nickel’ (40–50%) and ‘high-nickel’ (72–80%) [31,32]. The

* Corresponding author.

E-mail address: christina.byrka@gmail.com (C. Gritsenko).

<https://doi.org/10.1016/j.jmmm.2019.03.044>

Received 19 October 2018; Received in revised form 7 March 2019; Accepted 7 March 2019

Available online 08 March 2019

0304-8853/ © 2019 Published by Elsevier B.V.

‘High-nickel’ Permalloy has a small crystalline anisotropy, large initial permeability, and is usually used in traditional exchange bias systems [33–35]. The ‘Low-nickel’ Permalloy has higher crystalline anisotropy and larger saturation magnetization in comparison with the ‘high-nickel’ Permalloy. The ‘Low-nickel’ one is usually used in hard drives [31,36].

One of the ways to change the required properties of the exchange coupled systems is to use the trilayer structures instead of bilayers [37,38], where two ferromagnetic layers are separated by the antiferromagnetic one. Such structures can provide the step-wise hysteresis loops [39] due to two exchange-coupled interfaces with different energies. In this case the sequence of magnetization reversal of two FM layers is not obvious [27,40], and depends on a wide range of factors: technological parameters, materials, layer thicknesses etc.

Both the FM- and AFM-layer thicknesses play a crucial role for the exchange bias effect. As it was observed experimentally, at a constant FM-layer thickness the blocking temperature of exchange bias (the temperature at which the exchange bias becomes nonzero) decreases with decreasing antiferromagnetic layer thickness in both NiFe/IrMn and IrMn/NiFe structures [41]. Such a tendency is common and can be explained by usually used theoretical condition [37,42] for the existence of the exchange bias $K_{AFM} t_{AFM} > J_{EX}$ (Eq. (1)), where K_{AFM} is the anisotropy energy of an antiferromagnetic, t_{AFM} stands for an AFM-layer thickness, and J_{EX} is the interfacial exchange coupling energy.

The temperature dependence of the exchange bias is also affected by the ferromagnetic and antiferromagnetic layer thicknesses [43,44]. Generally, with decreasing the temperature in the region below blocking temperature the exchange bias increases [39,41], but the peak-like behavior depending on the layers thicknesses can be observed [45].

In this work, the FM/AFM/FM trilayer compositions with either low- or high- nickel Permalloy have been studied. In particular, the sequence of magnetization reversal of FM layers has been found to differ for the samples based on low- and high-nickel Permalloy in the temperature range from 80 K to 300 K.

2. Experimental details

The NiFe/IrMn/NiFe thin-film structures were fabricated by magnetron sputtering at an ambient temperature in Ar atmosphere with pressure of 3 mTorr. Magnetic field of 500 Oe was applied in plane of the substrate during the deposition process to induce the unidirectional anisotropy in samples. The substrate was Si/SiO₂ (1 0 0). The buffer Ta layer with a thickness of 30 nm was deposited onto the substrate to improve the growth of further layers. For each structure, the FM-layer that was deposited prior to the other one (i.e. onto the Ta buffer layer) is denoted as “bottom”. Accordingly, the FM layer that was deposited on top of the IrMn layer is denoted as “top”. The last layer of 30 nm of Ta was deposited on top of each sample to prevent them from the oxidation. We prepared two series of samples, one using ‘low-nickel’ Permalloy that is Ni₄₀Fe₆₀ (LNiPy), and the other using ‘high-nickel’ Permalloy that is Ni₇₅Fe₂₅ (HNiPy). Two targets of separated Ni and Fe were used for co-deposition of NiFe alloys. The target Ir₄₅Mn₅₅ alloy was used for deposition of an antiferromagnetic layer. The layers thicknesses were set by the deposition time with the deposition rates

estimated from the measurements of the thickness of the calibration samples by the Rutherford backscattering method. The NiFe layers were fabricated to have thickness of 10 nm, while the thickness of IrMn layers was varied to be 2, 4 or 10 nm.

The study of the samples structural properties was carried out using transmission electron microscopy (TEM) using Hitachi HT7700 microscope at the accelerating voltage of 100 kV. Cross-section pieces of samples were prepared using a Hitachi FB2100 (FIB) single-beam focused ion beam system. The magnetic properties of the samples were investigated using a Vibrating Sample Magnetometer (VSM, Lake Shore, Model 7400). The hysteresis loops for each sample were measured for in-plane geometry with the magnetic field of the VSM oriented along the induced unidirectional anisotropy, in the temperature range from 80 K to 300 K.

3. Results and discussion

The TEM cross-sectional images, presented in Fig. 1, show that the interfaces between the NiFe layers and IrMn are smooth except the one between the bottom LNiPy and IrMn. In the case of the LNiPy/IrMn interface, the partial intermixing of layers is observed (marked as dashed lines). It can occur because the LNiPy grows with a large grain size [46,47]. The large grain size of LNiPy causes the enhanced roughness of the LNiPy layer surface. Assuming the IrMn layer grains to be smaller than LNiPy grains [48–50], it can possibly fill the gaps between the LNiPy grains. Meanwhile, a characteristic size of the HNiPy grains is comparable to that of the IrMn grains [50].

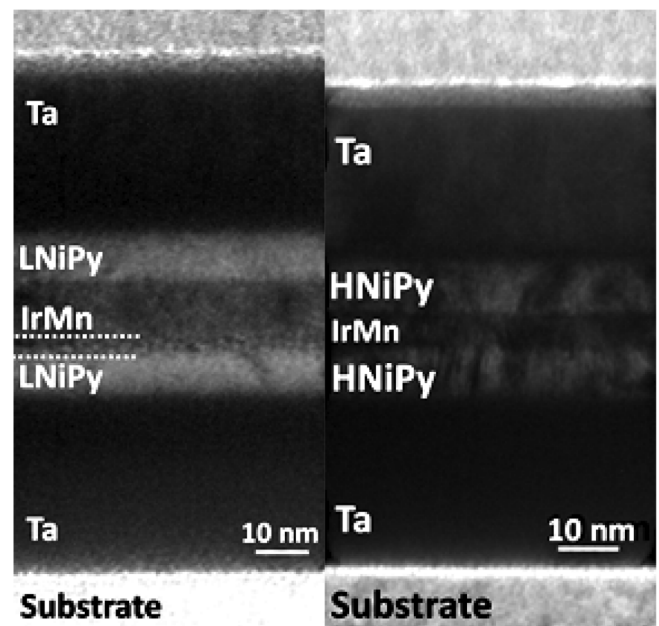


Fig. 1. TEM cross-sectional images for the samples LNiPy(10 nm)/IrMn (10 nm)/LNiPy(10 nm) and HNiPy(10 nm)/IrMn(5 nm)/HNiPy(10 nm).

Fig. 2(a) shows the hysteresis loops for the samples NiFe/IrMn (10 nm)/NiFe with LNiPy (red curve) and HNiPy (black curve). As it can be seen, the loops exhibit the step-like shape. The steps in the black hysteresis loop are of equal height because the two FM layers of HNiPy are of the same 10 nm thickness, as it was confirmed by the TEM. However, the red hysteresis loop has non-equal heights of the steps in the descending branch: the bottom step is of smaller height than the top one. This may be caused by the decrease of the thickness of the bottom FM layer due to its partial intermixing with the IrMn layer, which was demonstrated earlier [46,50], and is shown in Fig. 1. It can be concluded that the top FM layer reverses prior to the bottom one.

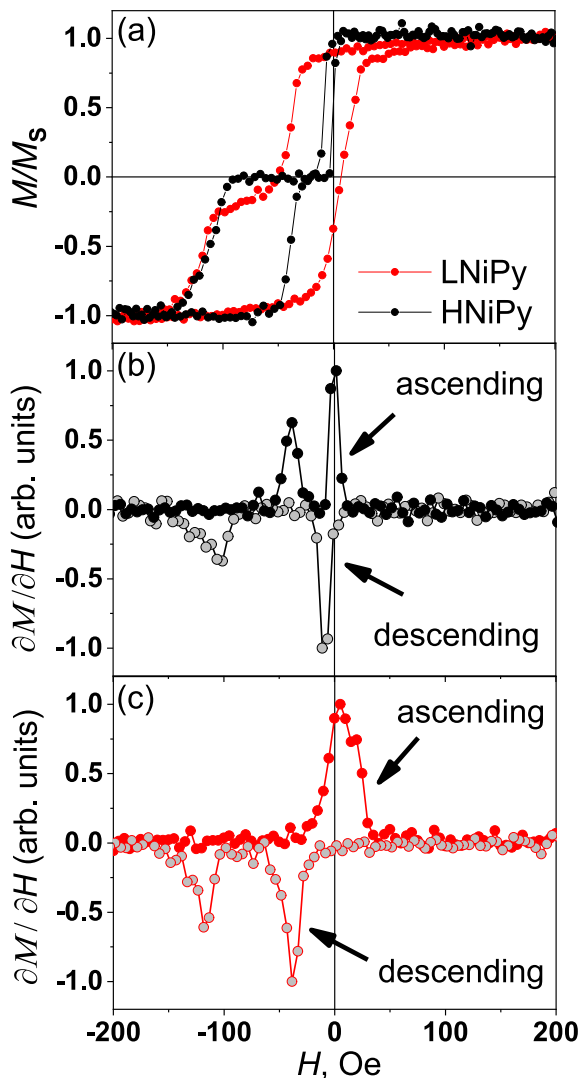


Fig. 2. (a) Hysteresis loops for LNiPy (red lines) and HNiPy (black lines) NiFe/IrMn(10 nm)/NiFe samples, obtained along the unidirectional anisotropy axis; differential susceptibility vs magnetic field for the HNiPy (b) and LNiPy (c) samples.

The fact that the bottom FM layer reverses prior to the top one in the HNiPy sample with the equal heights of the subloops can be confirmed by the coercivities and exchange bias fields for the top and bottom subloops that correlate perfectly with the coercivities and exchange bias fields of the separate HNiPy/IrMn and IrMn/HNiPy structures [51]. Thus, the difference in magnetization reversal sequence for the HNiPy and LNiPy samples is observed under changing the magnetic field from H_S to $-H_S$ (descending branch).

To trace the sequence of magnetization reversal of ferromagnetic layers under changing the magnetic field from $-H_S$ to H_S , in Fig. 2(b),

(c) the differential susceptibility for the descending and ascending branches of the hysteresis loops for the aforementioned samples is depicted. The magnetization reversal of the different ferromagnetic phases corresponds to the various peak heights [52]. The sequence of magnetization reversal is found to be different for descending and ascending branches for the HNiPy sample: bottom-top-top-bottom. For the LNiPy sample at the descending branch two ferromagnetic layers reverse one by one while at the ascending branch two ferromagnetic layers reverse in one magnetic field: top-bottom-both (in one direction top layer then bottom one and in the opposite direction both layers switch simultaneously). It may be associated with additional pinning mechanism in reversed magnetic field.

This dependence of magnetization reversal sequence on Permalloy type persists for the thinner AFM layer systems. To observe this tendency, the samples magnetic properties were investigated at the temperatures down to 80 K. The typical hysteresis loops for the LNiPy and HNiPy NiFe/IrMn/NiFe samples with thicknesses of AFM-layer of 2 nm and 4 nm, at temperatures of 90 K, 200 K, and 300 K, are presented in Fig. 3.

For all samples the exchange bias is zero at room temperature. At 4 nm of IrMn layer in the HNiPy sample two ferromagnetic layers reverse together, while in the LNiPy sample they reverse in different fields keeping the order of the layers magnetization reversal the same as it was observed at the descending branch (Fig. 2(a)) for the LNiPy sample with 10 nm-AFM-layer. It happens because the two FM layers have different coercivities due to the different morphology of their surfaces, whereas the exchange bias is also zero. The confirmation of this suggested explanation can be found in Fig. 4, where the differential susceptibility is depicted. The sequence of the ferromagnetic layer magnetization reversal is top-bottom-top-bottom (Fig. 4(c)).

When the AFM layer thickness decreases from the 4 nm to 2 nm, the slope of hysteresis loops decreases (Fig. 3), as well as the width of the differential susceptibility peaks decreases (Fig. 4). This means that the contribution of the reversible switching (i.e. magnetic moments rotation) to the magnetization reversal decreases with increasing the AFM-layer thickness [52].

For all samples, when the temperature decreases, the coercive force and the exchange bias increases. The kinks in the hysteresis loops appear, indicating the separation of the two ferromagnetic phases, i.e. the two FM layers, due to the exchange bias effect, which has different influence on top and bottom layers as it was observed for 10 nm-AFM-layer samples. It can be more visible in the differential susceptibility vs H plotted in Fig. 4. The decrease of the temperature entails the peaks broadening, as well as the slope of hysteresis loops becomes bigger. According to [52], it can indicate that the contribution of the magnetic moment rotation into the magnetization reversal process increases compared to the domain wall motion. This can be explained in terms of thermal fluctuations model [53], from which it follows that the spin structure at the interfaces becomes more stable, because when temperature is decreased it reduces the thermal-fluctuations energy of AFM and FM atoms.

Magnetization reversal of the different ferromagnetic layers separated by the antiferromagnetic layer can be attributed to the differential susceptibility peaks with different heights. In other words, by the order in which the lower and higher peaks appear at the ascending and descending branches, one can judge the sequence of the magnetization reversal of the layers. Thus, at 90 K and 200 K the sequence of the magnetization reversal for two LNiPy layers of 2 nm and 4 nm-AFM-layer samples is the same as for 10 nm of AFM-layer thickness at room temperature (Fig. 2), i.e. top-bottom-both (in one direction top layer then bottom one and in the opposite direction both layers switch simultaneously). For the HNiPy samples with 4 nm of AFM-layer at 90 K and 200 K, the magnetization reversal sequence of the top and bottom FM-layers is the same as found for the HNiPy/IrMn/HNiPy sample with 10 nm of AFM layer at room temperature (Fig. 2(a)): bottom-top-top-bottom.

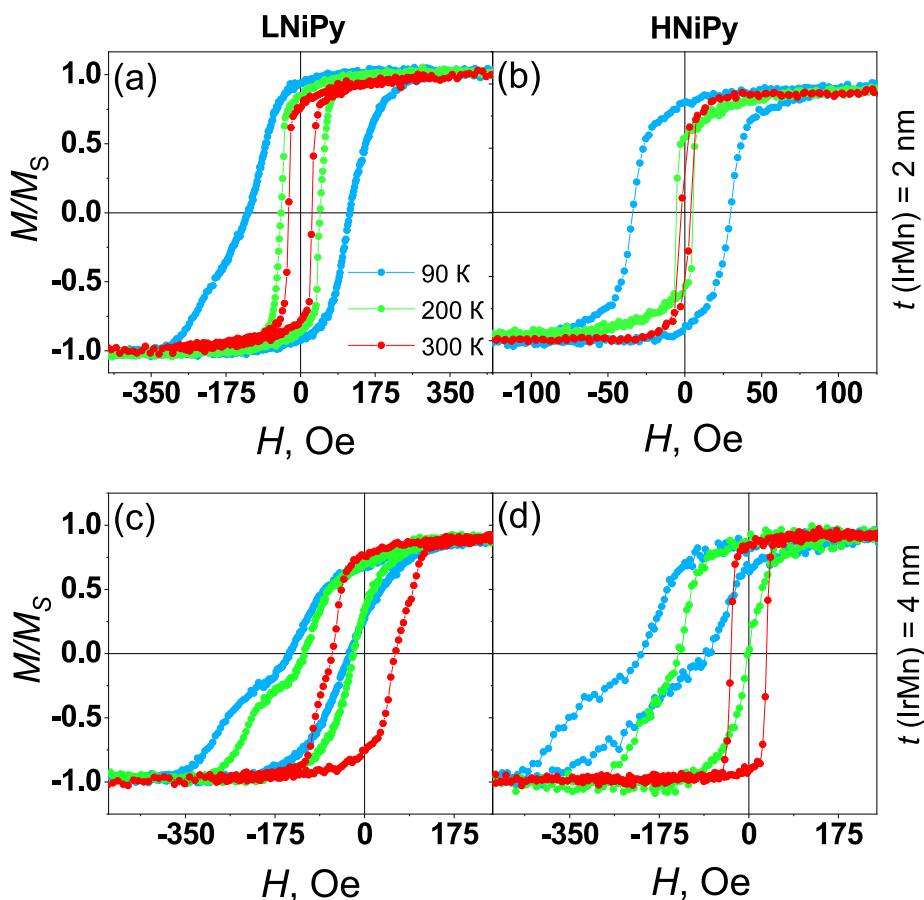


Fig. 3. Hysteresis loops obtained along the unidirectional anisotropy axis at different temperatures for NiFe/IrMn(t)/NiFe samples with LNiPy (a), (c) and HNiPy (b), (d).

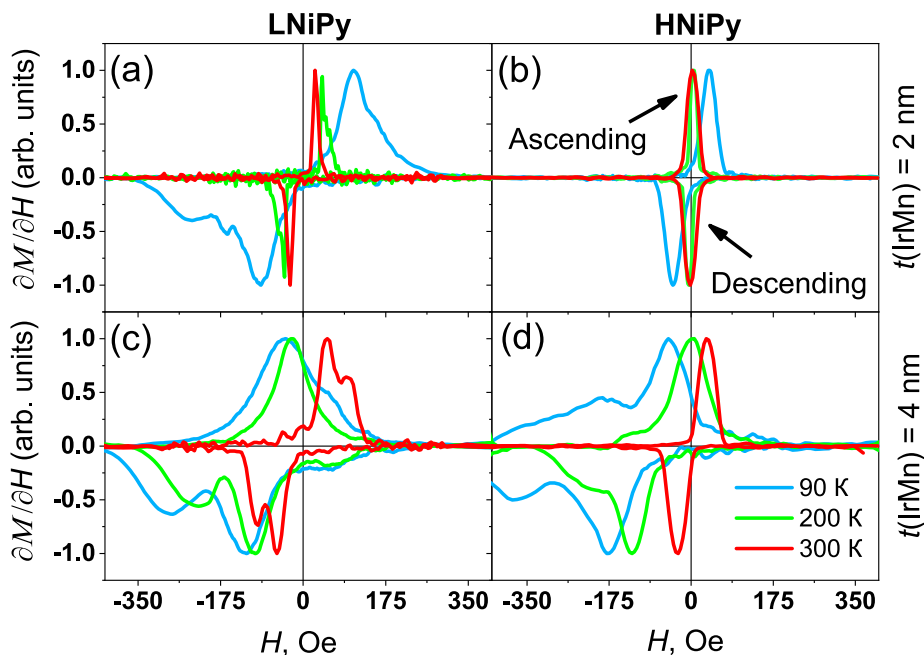


Fig. 4. The differential susceptibility vs magnetic field for NiFe/IrMn(t)/NiFe samples with LNiPy (a), (c) and HNiPy (b), (d) at different temperatures.

The dependences of the exchange bias and coercivity on the temperature are presented in Fig. 5. For the samples with IrMn layer thickness of 2 nm, the blocking temperatures were found to be 250 K for the LNiPy and 200 K for the HNiPy samples. For the samples with the antiferromagnetic layer thickness of 4 nm, the exchange bias was

observed at temperatures below 290 K. Thus, with the increase of the AFM-layer thickness the blocking temperature rises. Besides, the increase of AFM-layer thickness affects the exchange bias and coercivity curves vs temperature (Fig. 5) making them more convex. According to [54,55] the last two phenomena can indicate the change of interfacial

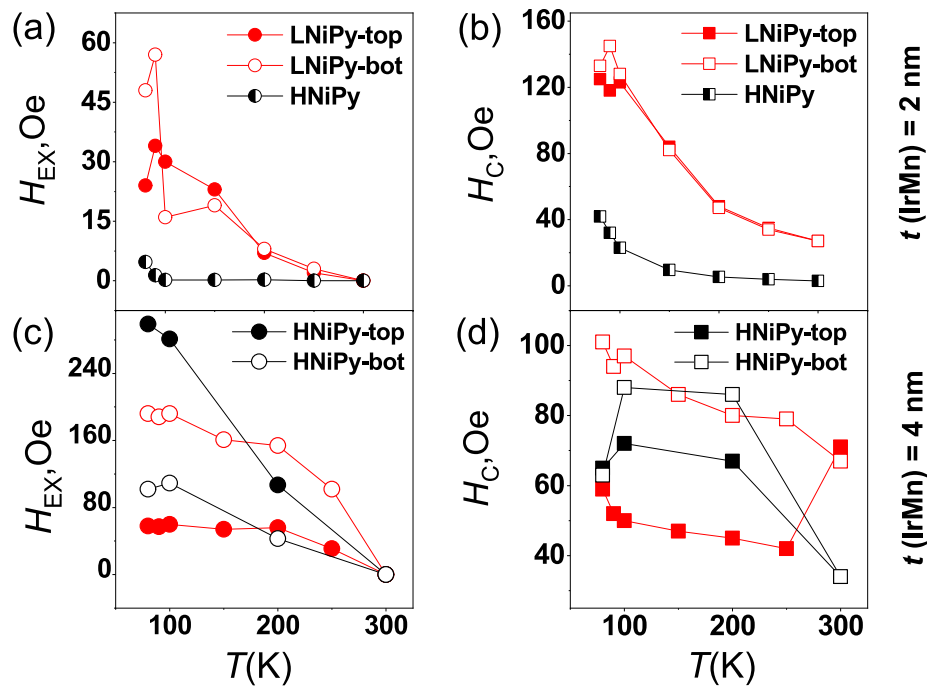


Fig. 5. Exchange bias (a), (c) and coercivity (b), (d) dependences on the temperature for the top and bottom FM-layers in NiFe/IrMn(t)/NiFe samples with LNiPy and HNiPy.

spin structure of the AFM and hence of interfacial exchange coupling type due to the increase of antiferromagnetic anisotropy constant. This hypothesis seems to be promising but requires further studies.

4. Conclusions

The studies of magnetic properties performed in the temperature range from 80 K to 300 K allowed us to determine the blocking temperatures of NiFe/IrMn/NiFe thin-film structures with the antiferromagnetic layer thicknesses of 2 nm and 4 nm, which do not exhibit the exchange bias effect at room temperature. The sequence of magnetization reversal for the two ferromagnetic layers has been determined to depend on the type of Permalloy. Thus, for the LNiPy samples the top FM-layer reverses prior to the bottom one. On the contrary, for the HNiPy samples the bottom FM-layer reverses prior to the top one. The aforementioned differences are supposedly caused by the morphological features at the interfaces between FM and AFM of the systems based on the LNiPy and HNiPy.

Acknowledgments

Ch. G. and M. G. acknowledge financial support by the Russian Foundation for Basic Research (RFBR grant № 17-32-50170). Ch. G. acknowledges the 5 top 100 Russian Academic Excellence Project at the Immanuel Kant Baltic Federal University. O.A.T. acknowledges support by the Grants-in-Aid for Scientific Research (Grant Nos. 17 K05511 and 17H05173) from MEXT, Japan, by the grant of the Center for Science and Innovation in Spintronics (Core Research Cluster), Tohoku University, by JSPS and RFBR under the Japan-Russian Research Cooperative Program. V.R. acknowledges the Ministry of Education and Science of the Russian Federation in the framework of government assignment 3.9002.2017/6.7. Electron microscopy examination was carried out at the Center for Collective Use of the Krasnoyarsk Scientific Center of the Siberian Branch of the Russian Academy of Sciences. We also thank Montserrat Rivas for helpful discussions.

References

- [1] W.H. Meiklejohn, C.P. Bean, New magnetic anisotropy, *Phys. Rev.* 102 (1956) 1413–1414.
- [2] R.E. Ching Tsang, Tsann Lin Fontana, D.E. Heim, V.S. Speriosu, B.A. Gurney, M.L. Williams, Design fabrication and testing of spin-valve read heads for high density recording, *IEEE Trans. Magn.* 30 (1994) 3801–3806, <https://doi.org/10.1109/20.333909>.
- [3] Z. Wei, A. Sharma, A.S. Nunez, P.M. Haney, R.A. Duine, J. Bass, A.H. MacDonald, M. Tsoi, Changing exchange bias in spin valves with an electric current, *Phys. Rev. Lett.* 98 (2007), <https://doi.org/10.1103/PhysRevLett.98.116603>.
- [4] Y. Jiang, T. Nozaki, S. Abe, T. Ochiai, A. Hirohata, N. Tezuka, K. Inomata, Substantial reduction of critical current for magnetization switching in an exchange-biased spin valve, *Nat. Mater.* 3 (2004) 361–364, <https://doi.org/10.1038/nmat1120>.
- [5] B.G. Park, J. Wunderlich, X. Martí, V. Holý, Y. Kurosaki, M. Yamada, H. Yamamoto, A. Nishide, J. Hayakawa, H. Takahashi, A.B. Shick, T. Jungwirth, A spin-valve-like magnetoresistance of an antiferromagnet-based tunnel junction, *Nat. Mater.* 10 (2011) 347–351, <https://doi.org/10.1038/nmat2983>.
- [6] Y.-T. Chen, The effect of interface texture on exchange biasing in Ni80Fe20/Ir20Mn80 system, *Nanoscale Res. Lett.* 4 (2009) 90–93, <https://doi.org/10.1007/s11671-008-9207-4>.
- [7] K. O'Grady, L.E. Fernandez-Outon, G. Vallejo-Fernandez, A new paradigm for exchange bias in polycrystalline thin films, *J. Magn. Magn. Mater.* 322 (2010) 883–899, <https://doi.org/10.1016/j.jmmm.2009.12.011>.
- [8] G. Vinai, J. Moritz, S. Bandiera, I.L. Prejbeanu, B. Dieny, Large exchange bias enhancement in (Pt(or Pd)/Co)/IrMn/Co trilayers with ultrathin IrMn thanks to interfacial Cu dusting, *Appl. Phys. Lett.* 104 (2014), <https://doi.org/10.1063/1.4872265>.
- [9] J. Nogués, D. Lederman, T.J. Moran, I.K. Schuller, K.V. Rao, Large exchange bias and its connection to interface structure in Fe2-Fe bilayers, *Cit. Appl. Phys. Lett.* 68 (1996) 44, <https://doi.org/10.1063/1.115819>.
- [10] K.W. Lin, T.C. Lan, C. Shueh, E. Skoropata, J. Van Lierop, Modification of the ferromagnetic anisotropy and exchange bias field of NiFe/CoO/Co trilayers through the CoO spacer thicknesses, *J. Appl. Phys.* 115 (2014) 1–5, <https://doi.org/10.1063/1.4861216>.
- [11] O. Zaharko, P.M. Oppeneer, H. Grimmer, M. Horisberger, H.C. Mertins, D. Abramsohn, F. Schäfers, A. Bill, H.B. Braun, Exchange coupling in Fe/NiO/Co film studied by soft x-ray resonant magnetic reflectivity, *Phys. Rev. B – Condens. Matter Phys.* 66 (2002) 1–10, <https://doi.org/10.1103/PhysRevB.66.134406>.
- [12] M. Fraune, U. Rü, G. Gü, S. Cardoso, P. Freitas, Size dependence of the exchange bias field in NiO/Ni nanostructures, *KOPS*, 2000.
- [13] A. Querejeta-Fernández, M. Parras, A. Varela, F. del Monte, M. García-Hernández, J.M. González-Calbet, Urea-melt assisted synthesis of Ni/NiO nanoparticles exhibiting structural disorder and exchange bias, *Chem. Mater.* 22 (2010) 6529–6541, <https://doi.org/10.1021/cm1017823>.
- [14] J.B. Yi, J. Ding, Z.L. Zhao, B.H. Liu, High coercivity and exchange coupling of

- Ni/NiO nanocomposite film, *J. Appl. Phys.* 97 (2005) 10K306, <https://doi.org/10.1063/1.1851424>.
- [15] I.N. Krivorotov, H. Yan, E. Dan Dahlberg, A. Stein, Exchange bias in macroporous Co/CoO, *J. Magn. Magn. Mater.* 226–230 (2001) 1800–1802, [https://doi.org/10.1016/S0304-8853\(00\)00934-3](https://doi.org/10.1016/S0304-8853(00)00934-3).
- [16] R. Cicheler, L.G. Pereira, T. Dias, J.E. Schmidt, C. Deranlot, F. Petroff, J. Geshev, Engineering double-shifted hysteresis loops in Co/IrMn/Cu/Co films, *Appl. Phys. Lett.* 95 (2009) 13–16, <https://doi.org/10.1063/1.3227840>.
- [17] W.A.A. Macedo, B. Sahoo, V. Kuncser, J. Eisenmenger, I. Felner, J. Nogués, K. Liu, W. Keune, I.K. Schuller, Changes in ferromagnetic spin structure induced by exchange bias in Fe/MnF₂ films, *Phys. Rev. B* 70 (2004) 5.
- [18] I. Suzuki, Y. Hamasaki, M. Itoh, T. Taniyama, Controllable exchange bias in Fe/metamagnetic FeRh bilayers, *Appl. Phys. Lett.* 105 (2014), <https://doi.org/10.1063/1.4900619>.
- [19] B. Altuncvahir, A.R. Koymen, Positive and negative exchange bias in CoNi/Gd/CoNi trilayers and CoNi/Gd bilayers, *J. Magn. Magn. Mater.* 261 (2003) 424–432, [https://doi.org/10.1016/S0304-8853\(02\)01493-2](https://doi.org/10.1016/S0304-8853(02)01493-2).
- [20] S.M. Rezende, M.A. Lucena, A. Azevedo, F.M. De Aguiar, J.R. Fermin, S.S.P. Parkin, Exchange anisotropy and spin-wave damping in CoFe/IrMn bilayers, *J. Appl. Phys.* 93 (2003) 7717–7719, <https://doi.org/10.1063/1.1543126>.
- [21] Y. Shen, Y. Wu, H. Xie, K. Li, J. Qiu, Z. Guo, Exchange bias of patterned NiFe/IrMn film, *J. Appl. Phys.* 91 (2002) 8001–8003, <https://doi.org/10.1063/1.1453322>.
- [22] S. Laureti, L. Del Bianco, B. Detlefs, E. Agostinelli, V. Foglietti, D. Peddis, A.M. Testa, G. Varvaro, D. Fiorani, Interface exchange coupling in a CoPt/NiO bilayer, *Thin Solid Films* 543 (2013) 162–166, <https://doi.org/10.1016/j.tsf.2012.12.115>.
- [23] J. Moritz, G. Vinai, B. Dieny, Large exchange bias field in (Pt/Co)₃/IrMn/Co trilayers with ultrathin IrMn layers, *IEEE Magn. Lett.* 3 (2012) 10–13, <https://doi.org/10.1109/LMAG.2012.2184794>.
- [24] L. Del Bianco, F. Spizzo, M. Tamisari, S. Laureti, Dependence of exchange bias on the field-cooled remanent magnetic state in Ni/NiO nanogranular samples, *Solid State Commun.* 151 (2011) 351–353, <https://doi.org/10.1016/j.ssc.2010.12.027>.
- [25] A. Maitre, D. Ledue, R. Patte, Interfacial roughness and temperature effects on exchange bias properties in coupled ferromagnetic/antiferromagnetic bilayers, *J. Magn. Magn. Mater.* 324 (2012) 403–409, <https://doi.org/10.1016/j.jmmm.2011.07.049>.
- [26] S.P. Hao, Y.X. Sui, R. Shan, L. Sun, S.M. Zhou, Exchange biasing in as-prepared Co/FeMn bilayers and magnetic properties of ultrathin single layer films, *Thin Solid Films* 485 (2005) 212–217, <https://doi.org/10.1016/j.tsf.2005.03.019>.
- [27] N. Nguyen Phuoc, N.P. Thuy, N.A. Tuan, L.T. Hung, N.T. Thanh, T. Nam, Coexistence of positive and negative exchange bias in CrMn/Co bilayers, *J. Magn. Magn. Mater.* 298 (2006) 43–47, <https://doi.org/10.1016/j.jmmm.2005.03.006>.
- [28] C. García, J.M. Florez, P. Vargas, C.A. Ross, Asymmetrical giant magnetoimpedance in exchange-biased NiFe, *Appl. Phys. Lett.* 96 (2010) 18–20, <https://doi.org/10.1063/1.3446894>.
- [29] C. Gritsenko, A. Omelyanchik, A. Berg, I. Dzhan, N. Chechenin, O. Dikaya, O.A. Tretiakov, V. Rodionova, Inhomogeneous magnetic field influence on magnetic properties of NiFe/IrMn thin film structures, *J. Magn. Magn. Mater.* 475 (2019) 763–766, <https://doi.org/10.1016/J.JMMM.2018.10.013>.
- [30] M.Y. S. X. Wang*, N. X. Sun*, S. Yabukami†, Properties of a new soft magnetic material, *Nature*. 407 (2000).
- [31] C. Tannous, R.L. Comstock, Springer Handbook of Electronic and Photonic Materials, 2017. doi:10.1007/978-3-319-48933-9.
- [32] E.S. Borovik, V.V. Ereyomenko, A.S. Milner, Lectures on Magnetism, FIZMATLIT, Moscow, 2005.
- [33] C. Liu, C. Yu, H. Jiang, L. Shen, C. Alexander, G.J. Mankey, Effect of interface roughness on the exchange bias for NiFe/FeMn, *J. Appl. Phys.* 87 (2000) 6644–6646, <https://doi.org/10.1063/1.372797>.
- [34] V.P. Nascimento, E.C. Passamani, A.D. Alvarenga, F. Pelegrini, A. Biondo, E. Baggio, Saitovitch, influence of the roughness on the exchange bias effect of NiFe/FeMn/NiFe trilayers, *J. Magn. Magn. Mater.* 320 (2008) 272–274, <https://doi.org/10.1016/j.jmmm.2008.02.059>.
- [35] F. Xu, Z. Liao, Q. Huang, N.N. Phuoc, C.K. Ong, S. Li, Characteristics of NiFe/IrMn/NiFe Trilayers, 47 (2011) 3486–3489.
- [36] N. Robertson, H.L. Hu, Ching Tsang, High performance write head using NiFe 45/55, *IEEE Trans. Magn.* 33 (1997) 2818–2820, <https://doi.org/10.1109/20.617741>.
- [37] J. Nogués, I.K. Schuller, Exchange bias, *J. Magn. Magn. Mater.* 192 (1999) 203–232, [https://doi.org/10.1016/S0304-8853\(98\)00266-2](https://doi.org/10.1016/S0304-8853(98)00266-2).
- [38] P.N. Lapa, I.V. Roshchin, J. Ding, J.E. Pearson, V. Novosad, J.S. Jiang, A. Hoffmann, Magnetoresistive detection of strongly pinned uncompensated magnetization in antiferromagnetic FeMn, *Phys. Rev. B* 95 (2017) 1–6, <https://doi.org/10.1103/PhysRevB.95.020409>.
- [39] G. Malinowski, M. Hehn, S. Robert, O. Lenoble, A. Schuhl, P. Panissod, Magnetic origin of enhanced top exchange biasing in Py/IrMn/Py multilayers, *Phys. Rev. B* 68 (2003) 184404, <https://doi.org/10.1103/PhysRevB.68.184404>.
- [40] D.L. Cortie, Y.W. Ting, P.S. Chen, X. Tan, K.W. Lin, F. Klöse, Enhancement of the magnetic interfacial exchange energy at a specific interface in NiFe/CoO/Co trilayer thin films via ion-beam modification, *J. Appl. Phys.* 115 (2014), <https://doi.org/10.1063/1.4865569>.
- [41] X.Y. Lang, W.T. Zheng, Q. Jiang, Dependence of the blocking temperature in exchange biased ferromagnetic/antiferromagnetic bilayers on the thickness of the antiferromagnetic layer, *Nanotechnology* 18 (2007), <https://doi.org/10.1088/0957-4484/18/15/155701>.
- [42] F. Radu, H. Zabel, Exchange bias effect of ferro-/antiferromagnetic heterostructures, in: S. Bader, H. Zabel (Eds.), *Magn. Heterostruct.*, 1st ed., Springer, Berlin, 2008: pp. 97–184. doi:10.1007/978-3-540-73462-8.
- [43] M. Ali, C.H. Marrows, M. Al-Jawad, B.J. Hickey, A. Misra, U. Nowak, K.D. Usadel, Antiferromagnetic layer thickness dependence of the IrMn/Co exchange-bias system, *Phys. Rev. B* 68 (2003) 214420, <https://doi.org/10.1103/PhysRevB.68.214420>.
- [44] J.P. King, J.N. Chapman, M.F. Gillies, J.C.S. Kools, Magnetization reversal of NiFe films exchange-biased by IrMn and FeMn, *J. Phys. D: Appl. Phys.* 34 (2001) 528–538, <https://doi.org/10.1088/0022-3727/34/4/315>.
- [45] K.M. Chui, D. Tripathy, a.O. Adeyeye, Temperature dependence of magnetotransport properties of Ni₈₀Fe₂₀/Fe₅₀Mn₅₀/Ni₈₀Fe₂₀ trilayers, *J. Appl. Phys.* 101 (2007) 09E512, <https://doi.org/10.1063/1.2709741>.
- [46] L.X. Phua, N.N. Phuoc, C.K. Ong, Investigation of the microstructure, magnetic and microwave properties of electrodeposited Ni_xFe_{1-x} (x = 0.2–0.76) films, *J. Alloys Compd.* 520 (2012) 132–139, <https://doi.org/10.1016/j.jallcom.2011.12.164>.
- [47] X. Chen, H. Qiu, H. Qian, P. Wu, F. Wang, L. Pan, Y. Tian, Characteristics of Ni x Fe 100Å films deposited on SiO₂/Si(1 0 0) by DC magnetron co-sputtering, *Vacuum* 75 (2004) 217–223, <https://doi.org/10.1016/j.vacuum.2004.03.001>.
- [48] K.-M.H. Lensen, A.E.M. De Veirman, J.J.T.M. Donkers, Inverted spin valves for magnetic heads and sensors, *J. Appl. Phys.* 81 (1997) 4915–4917, <https://doi.org/10.1063/1.364818>.
- [49] H.N. Fuke, K. Saito, M. Yoshikawa, H. Iwasaki, M. Sashiki, Influence of crystal structure and oxygen content on exchange-coupling properties of IrMn/CoFe spin-valve films, *Appl. Phys. Lett.* 75 (1999) 3680–3682, <https://doi.org/10.1063/1.125427>.
- [50] I. Dzhan, N. Chechenin, K. Chichay, V. Rodionova, Dependence of exchange coupling on antiferromagnetic layer thickness in NiFe/CoO bilayers, *ACTA Phys. Pol. A* 83 (2015) 6822–6824, <https://doi.org/10.1063/1.367863>.
- [51] C. Gritsenko, I. Dzhan, G. Babaytsev, N. Chechenin, V. Rodionova, Exchange bias and coercivity fields as a function of the antiferromagnetic layer thickness in bi- and tri-layered thin-films based on IrMn and NiFe, *Phys. Procedia* 82 (2016) 51–55, <https://doi.org/10.1016/j.phpro.2016.05.010>.
- [52] J.C. Martínez-García, M. Rivas, D. Lago-Cachón, J.A. García, First-order reversal curves analysis in nanocrystalline ribbons, *J. Phys. D: Appl. Phys.* 47 (2014) 015001, <https://doi.org/10.1088/0022-3727/47/1/015001>.
- [53] D. Ledue, A. Maitre, F. Barbe, L. Lechevallier, Temperature dependence of the exchange bias properties of ferromagnetic/antiferromagnetic polycrystalline bilayers, *J. Magn. Magn. Mater.* 372 (2014) 134–140, <https://doi.org/10.1016/j.jmmm.2014.07.021>.
- [54] C. Hou H. Fujiwara K. Zhang A. Tanaka Y. Shimizu Temperature dependence of the exchange-bias field of ferromagnetic layers coupled with antiferromagnetic layers *Phys. Rev. B* 63 2 2000 10.1103/PhysRevB.63.024411 <https://link.aps.org/doi/10.1103/PhysRevB.63.024411>
- [55] J.-G. Hu, G. Jin, A. Hu, Y.-Q. Ma, Temperature dependence of exchange bias and coercivity in ferromagnetic/antiferromagnetic bilayers, *Eur. Phys. J. B* 40 (2004) 265–271, <https://doi.org/10.1140/epjb/e2004-00272-0>.